Supporting Information

Ambient Synthesis of Nanomaterials by in situ Heterogeneous Metal/Ligand reactions

Boyce S. Chang,[1,2] *Brijith Thomas,*[2,3] *Jiahao Chen,*[1] *Ian D. Tevis,*[1] *Paul Karanja,*[1] *Simge Çınar,*[1] *Amrit Venkatesh,*[2,3] *Aaron J. Rossini,*[2,3]* *Martin M. Thuo*[1]*

[1]Department of Materials Science and Engineering, Iowa State University, 2220 Hoover Hall, Ames, IA 50011 USA

[2]US DOE Ames Laboratory, Ames, Iowa, USA, 50011

[3]Department of Chemistry, Iowa State University, 1605 Gilman Hall, Ames, IA 50011 USA

Materials. Glacial acetic (99.7%, Fisher Scientific), eutectic gallium-indium (99.99%, Sigma Aldrich), Gallium (99.99%, Rotometals), Indium (99.99%, Rotometals), Field's metal (32.5% Bismuth, 51% Indium, and 16.5% Tin, Rotometals), ethanol (>99.2%, Decon Laboratories Inc.), deuterium oxide (99.9 atom% D, Sigma Aldrich). Aluminum (ca 99%, US DOE Ames Laboratory), Nickel-Aluminum alloy (Ni95%-Al5%, US DOE Ames Laboratory).

Detailed Methods

Solid-State NMR Spectroscopy. All solid-state NMR experiments were performed with a 9.4 T Bruker Avance III HD spectrometer. MAS experiments were performed using a Bruker 1.3 mm HX probe; the MAS rate was 50 kHz unless mentioned otherwise. Some static $^{69/71}$Ga solid-state NMR experiments were performed using a 4.0 mm HX static probe. ^{1}H and ^{13}C chemical shifts were referenced to neat tetramethylsilane via an external secondary standard of adamantane. ^{2}H

chemical shifts and $^{69/71}$Ga chemical shifts were referenced with respect to proton chemical shifts by the recommended relative frequency scale.[1] The 50 kHz MAS ^{1}H SSNMR spectrum was acquired with a rotor synchronized spin echo pulse sequence ($\pi/2$-τ_r-π-τ_r) with 8 scans and a 60 second recycle delay. The 50 kHz MAS ^{2}H solid-state NMR spectrum of **1** synthesized in D_2O was acquired with a rotor synchronized solid echo pulse sequence ($\pi/2$-τ_r-$\pi/2$-τ_r) with 1024 scans, a 10.0 s recycle delay and low power 16 kHz continuous wave ^{1}H decoupling. The ^{1}H-detected ^{13}C cross-polarization HETCOR spectrum was acquired with a forwards and backwards cross-polarization pulse sequence.[2] A 2.5 ms contact time was used for the forwards and backwards cross-polarization steps. During cross-polarization, the ^{1}H pulse power was linearly ramped[3] from 110 kHz to 138 kHz and the ^{13}C rf field was fixed at ca. 74 kHz. The 2D spectrum was acquired with 4 scans per increment, a recycle delay of 2.5 s, 1024 t_1 increments, and a t_1 increment of 40.0 μs. During the indirect dimension ^{13}C evolution period, low power continuous wave ^{1}H decoupling was applied with an rf field of *ca*. 16 kHz. Quadrature detection in the indirect dimension was achieved with the States-TPPI procedure.[4-5]

^{71}Ga pulse widths were calibrated with a 1.0 M aqueous solution of $GaCl_3$, while ^{13}C pulse calibrations were used to calibrate ^{69}Ga pulses. Static $^{69/71}$Ga SSNMR spectra were acquired with the WURST-QCPMG pulse sequence.[6-7] Continuous wave ^{1}H hetero-nuclear decoupling with an rf field of 50 kHz was applied for the duration of the static WURST-QCPMG experiments. The ^{71}Ga SSNMR spectrum was acquired with 25 μs WURST pulses with a total frequency sweep width of 600 kHz and a single transmitter offset. Two spectra acquired with WURST pulses of opposite sweep direction were co-added and each spectrum was acquired with 512 scans and a 0.5 s recycle delay. 60 echoes of 100 μs duration each were acquired. All ^{69}Ga SSNMR sub-spectra were acquired with 25 μs WURST pulses which swept over 800 kHz. The variable offset cumulative spectra (VOCS) procedure[8] was used to acquire the total ^{69}Ga SSNMR spectrum. The total spectrum was formed by co-adding the 9 sub-spectra acquired by incrementing the transmitter frequency in steps of 180 kHz. For each transmitter offset two WURST-QCPMG spectra were acquired with opposite pulse sweep directions. Each sub-spectrum was acquired with 1200 scans and a 0.5 s recycle delay. The MAS ^{71}Ga SSNMR spectrum was acquired with an MAS frequency of 50 kHz with a rotor synchronized QCPMG pulse sequence with 1128 scans and a 0.5 s recycle delay.[9-10] The central transition selective $\pi/2$ and π pulses were 0.94 μs and 1.88 μs, respectively. The MAS QCPMG SSNMR spectrum was

obtained with 40 spin echoes, each of which was 200 μs in duration. Echo reconstructed MAS and static ^{71}Ga SSNMR spectra were formed from the CPMG spectra by co-adding each of the spin echoes in the CPMG echo-train together, then Fourier transforming the resulting whole spin echo.[11-12]

For the formic acid and 50% acetic acid solution coordination polymers, static $^{69/71}$Ga SSNMR spectra were acquired with a Bruker 4 mm HX static probe using the WURST-QCPMG pulse sequence and VOCS procedure. 25 μs WURST pulses with a total frequency sweep width of 600 kHz were employed and two WURST-QCPMG spectra were obtained at each transmitter position with opposite sweep directions. An rf field of ca. 20 kHz was used for the WURST pulses while the ^{1}H decoupling rf field was set to ca. 60 kHz for acquiring ^{71}Ga SSNMR spectra and ca. 30 kHz for acquiring ^{69}Ga solid-state NMR spectra. The duration of each echo was set to 200 μs and 100 μs respectively, for ^{71}Ga and ^{69}Ga WURST-QCPMG spectra. The number of echoes in the ^{71}Ga and ^{69}Ga QCPMG echo-trains were 70 and 50, respectively in case of the Formic acid polymer and 50 and 35, respectively for the 50% Acetic acid polymer. The total spectrum was obtained by co-adding multiple sub-spectra acquired by incrementing the transmitter frequency in steps of 150 kHz. In each case, the transmitter was stepped on either side of the 'zero' position until no signal could be observed. Recycle delays of 0.25 s and 0.1 s were used to obtain ^{71}Ga and ^{69}Ga WURST QCPMG spectra, respectively with 256 scans for the formic acid sample and 512 scans for the 50% Ac sample.

The 2D ^{1}H-^{71}Ga dipolar hetero-nuclear multiple-quantum correlation (D-HMQC) spectrum was acquired using the previously described constant-time pulse sequence.[13-14,20] The 2D spectrum was acquired with 32 scans per t_1 increment, a recycle delay of 1.0 s, 160 total t_1 increments and the t_1 increment was 1.25 μs. In order to increment t_1 asynchronously with respect to the rotor period, the spin echo block in the center of the D-HMQC pulse sequence was fixed to a rotor synchronized total period of 120 μs and the π/2 pulses on ^{71}Ga were incremented outwards from the central ^{1}H π pulse.[15] Short, high power CT selective 0.61 μs π/2 pulses were applied to ^{71}Ga in the HMQC pulse sequence in order to obtain broadband excitation. Supercycled $R4^2_1$ dipolar recoupling[14, 16] was applied for a total duration of 1280 μs (32 rotor cycles for excitation and reconversion). Quadrature detection in the indirect dimension was achieved with the States-TPPI procedure.[4-5] Analytical simulations of static and MAS $^{69/71}$Ga

SSNMR spectra were performed in the solid lineshape analysis (SOLA) module v2.2.4 included in the Bruker Topspin v3.2 software.

Other Instruments. Scanning electron micrographs were obtained using Zeiss Supra55VP field emission SEM and FEI Helios NanoLab G3 UC under immersion mode. X-ray photoelectron spectroscopy was performed using Thermo Scientific K-Alpha XPS. Infrared spectroscopy was performed using Perkin Elmer Frontier FT-MIR spectrometer in attenuated total reflectance (ATR) mode. The Rigaku Smartlab X-ray diffractometer was used to perform all powder x-ray diffraction experiments.

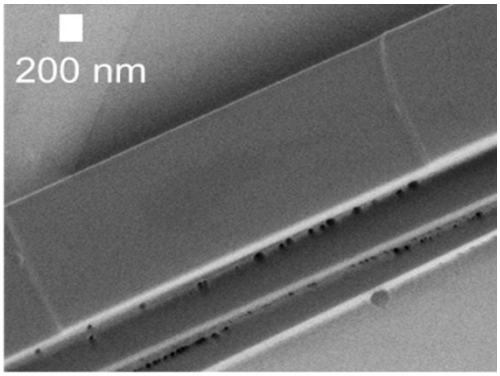

Figure S1. Step-like structures suggesting that the beams consist of stacked sheets.

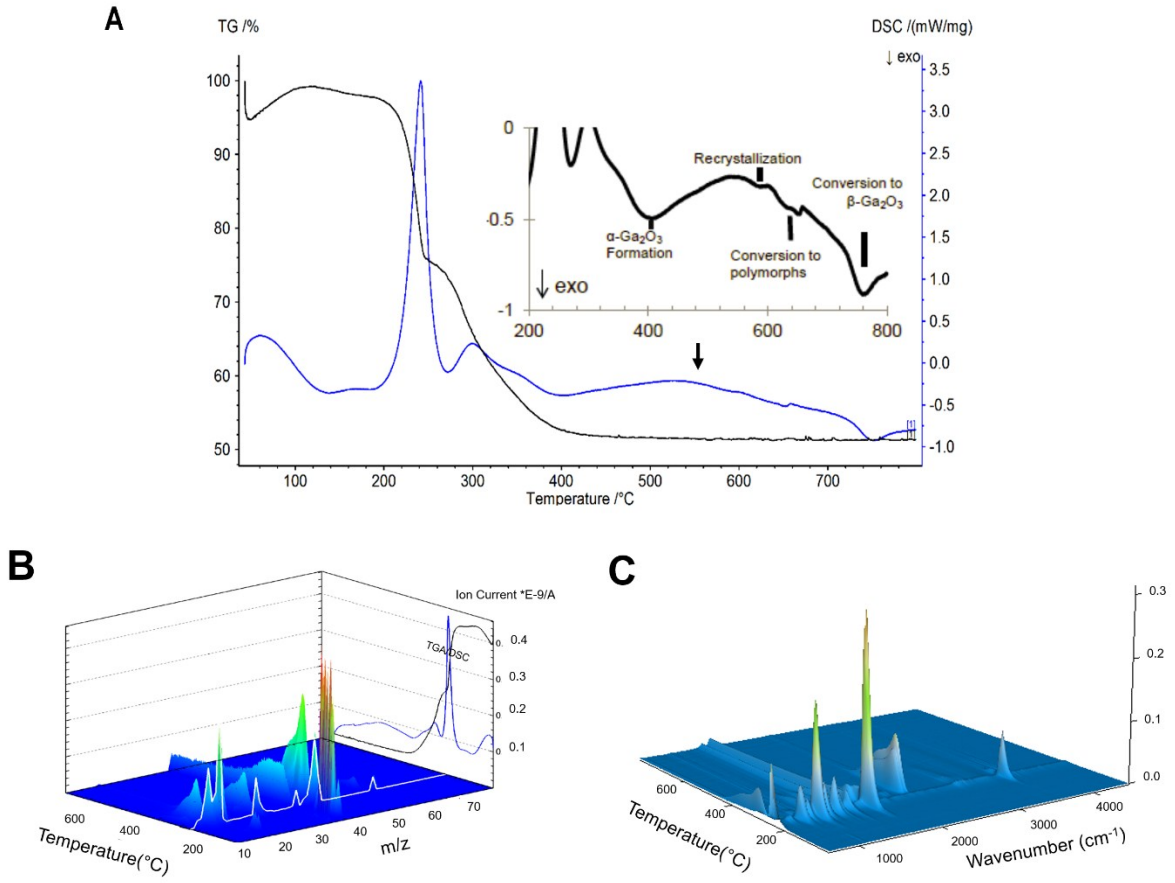

Figure S2. Characterization of heat treated nanobeams. (A) TGA and DSC showing two decomposition steps occurring from 188 to 240 °C and from 240 to ~446 °C and their corresponding endothermic peaks in the DSC. Expanded region of DSC highlighting the crystallization and conversion of the nanobeams to β-Ga_2O_3. (B) Mass spectrum of the gas evolved during the TGA experiment at 243 °C and 296 °C (C) FTIR of the gas evolved during TGA. The intense signal occur at the major events at 243 °C and 296 °C.

At the higher temperature degradation step the major product is carbon dioxide with its characteristic IR peaks at 2362 cm^{-1}. Additional minor products are acetic acid, acetate, water, and CO. The MS peaks at 58, 44, 38, 18, 15, and 12 m/z were attributed to $C_2O_2H_2^+$, CO_2^+, CO^+,

H_2O^+, CH_3^+, and C^+ respectively. The majority of the water loss occurs before 300 °C while more extensive decomposition of the acetates into carbon dioxide occurs around 300 °C.

FTIR and MS spectra shows that the first degradation product is acetic acid with the characteristic OH stretches around 3581 cm^{-1} from the trans-monomer acetic acid and C=O stretches around 1797 cm^{-1}. Additional peaks are observed at 1558 and 1448 cm^{-1} correspond to a non-protonated acetate. Finally, weak and broad water peaks are observed around 3311 cm^{-1}. The MS matches this assessment with a molecular ion peak at 60 m/z and fragmentation peaks at 44, 28, 18, 15 m/z corresponding to CO_2^+, CO^+, H_2O^+, and CH_3^+ respectively. The first degradation step could be a reaction along the close and strongly bound bridging OH groups that occur along the polymerization direction of the nanobeams. This inference is supported by both TGA-IR-MS and considering that a labile dative bond is necessary to complete the coordination sphere along the 1D chain.

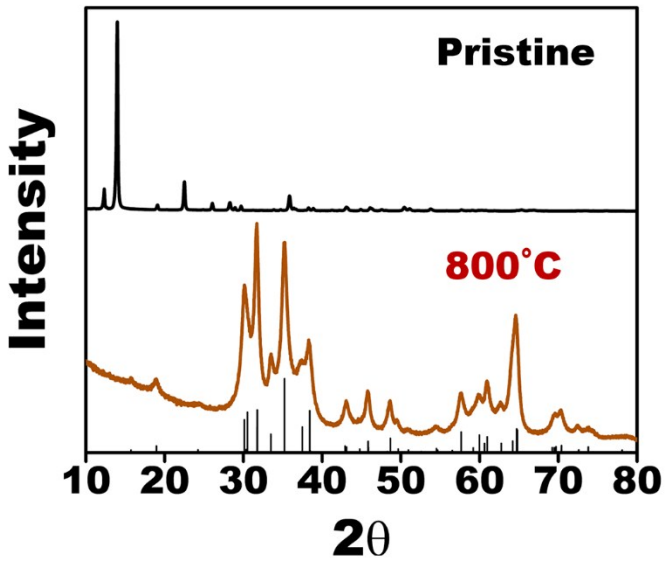

Figure S3. Powder X-ray diffraction before and after heat treatment at 800˚C, the material crystallizes into β-Ga_2O_3.

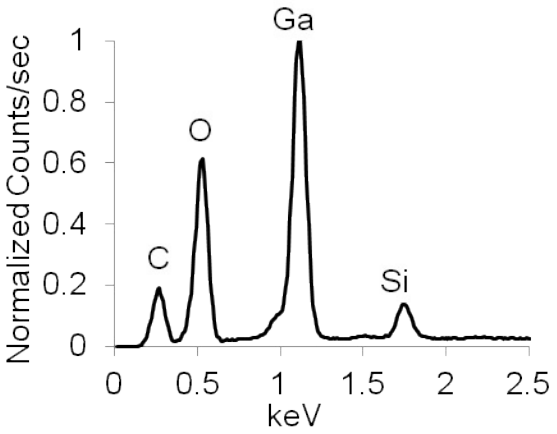

Figure S4. Elemental map created using Energy Dispersive X-ray spectrometry in an SEM showing the composition of the nanobeams is high in oxygen content. Si peaks originate from the Si wafer used as the substrate for imaging.

Infrared spectroscopy

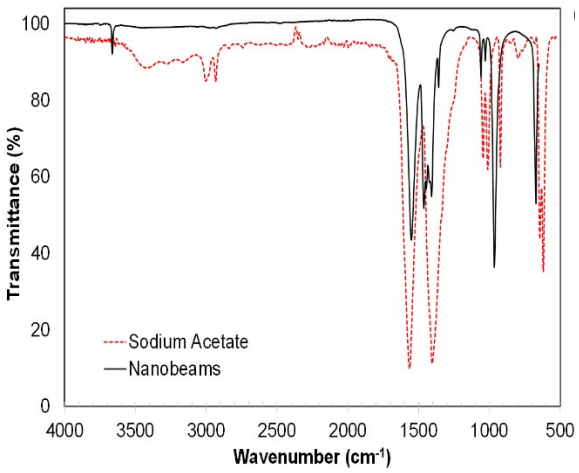

Figure S5. IR spectroscopy of nanobeam vs sodium acetate.

Acetic acid shows characteristic IR absorptions between 1300 – 1200 cm^{-1} and 1750 – 1700 cm^{-1} for C–O and C=O peaks, respectively. [17] Absence of these carboxylate peaks in FTIR spectra of nanobeams shown in Figure S5 indicates that all free carboxylate ions are washed out and interstitial acetic acid compounds are absent in the fabricated structure. Sodium acetate, which show absorptions at 1563 cm^{-1} and 1406 cm^{-1} corresponding to asymmetric and symmetric acetate stretching, respectively, was used as a reference.[17-18] The nanobeams have a strong CO_2 antisymmetric stretching peak at 1554 cm^{-1} and CO_2 symmetric stretching peaks at 1459 cm^{-1} and 1410 cm^{-1}, all of which are similar to the peak positions observed in sodium acetate. The wavenumber difference between the asymmetric and symmetric peaks in the nanobeams is 95 cm^{-1} (for the symmetric stretch at 1459 cm^{-1}) and 144 cm^{-1} (for the symmetric stretch at 1410 cm^{-1}). In sodium acetate this difference is 157 cm^{-1} which is slightly larger than for the nanobeams. This smaller frequency difference in the nanobeams can likely be attributed to stronger binding of the acetate ligands due to bridging or chelating binding. [24,25] It is also found out that adsorbed OH peaks on IR spectrum can be eliminated by washing the beam through acetone rather than ethanol (broad OH absorbance between 3000 cm^{-1} and 3600 cm^{-1} in Figure 3f-g).

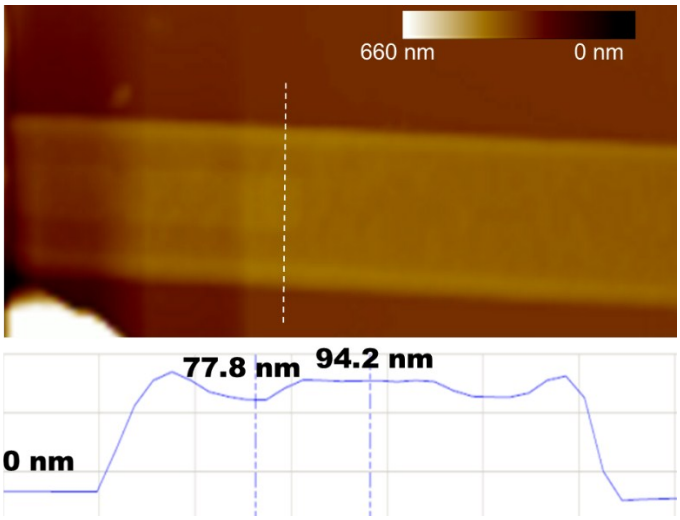

Figure S6. AFM topography images of a nanobeam demonstrating that the sides are curled.

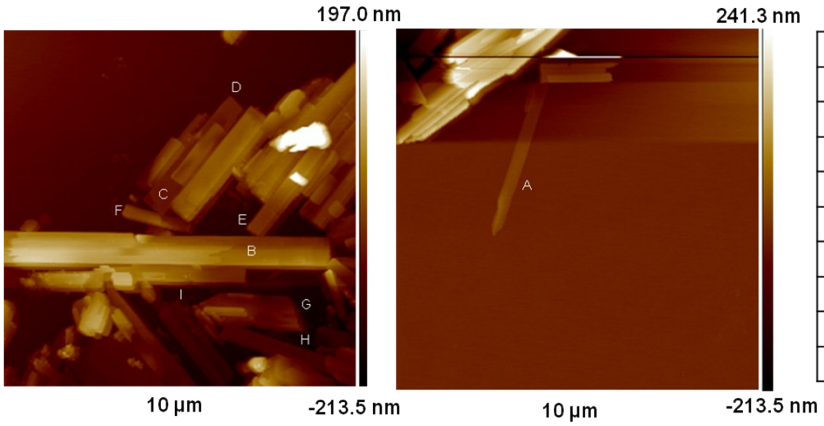

Label	Height (nm)	Step Height (nm)
A	30.3	-
B	131.3	11.4
C	47.6	12.3
D	49.2	-
E	83.5	-
F	79.9	-
G	71.3	-
H	54.6	-
I	73.4	-

Figure S7. Additional AFM topography images of nanobeams and a table of their measured height.

X-ray photoelectron spectroscopy

The gallium peak at 20.7 eV is consistent with a fully oxidized gallium to Ga^{3+}. There is, however, no peak around 18.7 eV consistent with the absence of elemental gallium from the EGaIn precursor. The oxygen peak at 532.0 eV is consistent with oxygen in organic compounds and not in metal oxides that are typically seen around 529-530 eV. Further details on the organic bond, however, is almost impossible to interpret because of broad overlapping peaks. The carbon content in the structure is confirmed with the peak at 288.9 eV, which can be attributed to C=O groups.[19]

Additional Details on the NMR Experiments Shown in Figure 3

The MAS ^{1}H solid-state NMR spectrum of coordination polymers obtained by etching of EGaIn in 5% acetic acid solution was obtained with an MAS frequency of 50 kHz is shown in the upper part of Figure 3a, and shows a single peak with an isotropic chemical shift of ca. 1.9 ppm. This chemical shift agrees well with the expected chemical shift for the methyl groups of acetate. Other distinct ^{1}H signals that could correspond to either hydroxyl protons or water included in lattice of nanobeams are not observed. For this reason, 50 kHz MAS ^{2}H solid-state NMR experiments on nanobeams grown in D_2O were performed (Figure 3a). Signals from the methyl group of acetate should be absent since the exchange of the methyl protons with ^{2}H will be very slow. Therefore, only signals from deuterated hydroxyl groups and any potential D_2O incorporated into the lattice will be observed. The isotropic region of the ^{2}H solid-state NMR spectrum shows a single peak visible at a frequency of ca. 2.6 ppm, which is assigned to deuterated hydroxyl groups coordinated to Ga. The ^{2}H peak position, however, is affected by the second order quadrupolar interaction so that the peak position does not correspond to the true ^{2}H chemical shift. By fitting the ^{2}H sideband manifold (inset, Figure 3a) the quadrupole parameters and real ^{2}H isotropic chemical shift can be determined. An isotropic ^{2}H chemical shift of 1.9 ppm is determined from the fit of the isotropic peak and sideband manifold. Therefore, the ^{1}H chemical shift of the hydroxyl groups and acetate methyl protons are coincident, and this explains why only a single broad signal was observed in the ^{1}H NMR spectrum.

A proton detected ^{1}H-^{13}C dipolar HETCOR spectrum shown in Figure 3b confirms the presence of acetate anions in the coordination polymer. The ^{13}C dimension shows two signals with chemical shifts of 24.5 ppm and 179.0 ppm which are characteristic of the methyl group and the carboxylic acid carbon of the acetate ligands coordinated to gallium. The ^{13}C dimension only shows the presence of one set of ^{13}C signals. This is in agreement with the IR results that suggest that all acetate ligands within the lattice around are bound to Ga, i.e., there are no interstitial non-coordinating acetate/acetic acid as has previously been observed in a Ga hydroxide-acetate coordination polymer.[20] The observation of a single set of signals also suggests that all acetate ligands within the lattice are equivalent. This is consistent with the crystal structure existing as a symmetric repeating coordination polymer (*vide infra,* Figure 1A).

Gallium possesses two highly abundant NMR active nuclei ^{69}Ga (N.A. = 60.1 %) and ^{71}Ga (N.A. = 39.9 %). Both are quadrupolar $I = 3/2$ nuclei with substantial quadrupole moments. ^{71}Ga gives rise to narrower solid-state NMR powder patterns due to its higher magnetogyric ratio ($\upsilon_0(^{71}Ga)$ = 122.1 MHz at 9.4 T) and its smaller quadrupole moment and is usually the preferred isotope for NMR. Previous $^{69/71}Ga$ solid-state NMR spectra have been acquired for oxides,[8, 21-23] coordination polymers, [24] metal-organic frameworks (MOFs), [25-26] organometallic dyes, [27] and inorganic cluster compounds.[28] The observed $^{69/71}Ga$ NMR powder patterns frequently span hundreds of kHz due to substantial broadening by the second-order quadrupolar interaction. The large breadths of the $^{69/71}Ga$ solid-state NMR spectra often necessitate special wide line solid-state NMR techniques.[8, 29]

The static (i.e., stationary sample) and MAS ^{71}Ga SSNMR spectra of nanobeams are shown in Figure 3c. The static ^{69}Ga SSNMR spectrum is shown in Figure S8. We have acquired spectra of both Ga isotopes in order to obtain accurate electric field gradient (EFG) and chemical shift (CS) tensor parameters from simulations of the experimental spectra (Table S1). The spectra can be satisfactorily fit with a single site with a large quadrupolar coupling constants (C_Q) of 16.9 MHz and 26.9 MHz, for ^{71}Ga and ^{69}Ga, respectively, and a quadrupolar asymmetry parameter (η_Q) of 0.14. An MAS ^{71}Ga SSNMR spectrum was also acquired with a fast MAS frequency of 50 kHz (Figure 3c). The MAS ^{71}Ga SSNMR spectrum confirms that the fits of the static NMR spectra are accurate and enables a more precise measurement of the isotropic chemical shift (δ_{iso}). Finally, a 2D ^{1}H-^{71}Ga constant time D-HMQC dipolar correlation spectrum

directly confirms the spatial proximity of Ga to the acetate and/or hydroxyl ligands (Figure 3d).[30-31]

Table S1. Chemical shift and electric field gradient tensor parameters obtained from simulations of ^{71}Ga and ^{69}Ga static and MAS solid-state NMR spectra.

NMR Parameter[a]	^{71}Ga/^{69}Ga
δ_{iso} (ppm)	–15(20)
C_Q (MHz)[b]	16.9(3) / 26.9(3)
η_Q	0.14(5)
Ω (ppm)[c]	340
κ	0.53
α (°)	–10
β (°)	25
γ (°)	30

[a]The CS tensor is defined by three principal components ordered such that $\delta_{11} \geq \delta_{22} \geq \delta_{33}$, $\delta_{iso} = (\delta_{11} + \delta_{22} + \delta_{33})/3$, $\Omega = \delta_{11} - \delta_{33}$ and $\kappa = 3(\delta_{22} - \delta_{iso})/\Omega$. The EFG tensor is described by three principal components ordered such that $|V_{11}| \leq |V_{22}| \leq |V_{33}|$, $C_Q = eQV_{33}/h$ and $\eta_Q = (V_{22} - V_{11})/V_{33}$. The Euler angles describe the relative orientations of the EFG and CS tensors. Uncertainties in experimental parameters are indicated in parentheses. [b]The C_Q values for ^{69}Ga and ^{71}Ga are directly proportional to the quadrupole moment of the nucleus, therefore, spectra from both nuclei were simulated simultaneously with the constraint, $C_Q(^{69}\mathrm{Ga}) = \left[Q(^{69}\mathrm{Ga})/Q(^{71}\mathrm{Ga})\right] \times C_Q(^{71}\mathrm{Ga}) = 1.59 \times C_Q(^{71}\mathrm{Ga})$. [c]The uncertainties associated with the CS and EFG tensor parameters and Euler angles are very large (±50%) and are included as adjustable parameters to improve the quality of the simulations. Acquisition of data at multiple magnetic fields could improve the uncertainties associated with these parameters.

On the basis of the EFG and CS tensor parameters extracted from the experimental $^{69/71}$Ga SSNMR spectra, several conclusions regarding the structure of 5% acetic acid coordination polymer can be made: *(i)* The determined isotropic chemical shift of –25 ppm is

similar to those previously reported for 6-coordinate Ga found in oxides and Ga phosphonate-hydroxide complexes. [21, 24] Note that 4-coordinate Ga typically possesses an isotropic chemical shift of ca. +200 ppm.[21-22] The measured δ_{iso} suggests that the Ga coordination environment in the coordination polymer must be 6-coordinate. *(ii)* The observation of a single Ga site in the NMR spectra suggests that the structure of coordination polymer must be symmetric so that all Ga sites within the lattice are equivalent; there should only be a single repeating unit within the coordination polymer chains. *(iii)* It is well known that the magnitude of C_Q depends upon the symmetry at the nuclear site, with spherically symmetric sites possessing small or vanishing C_Q and distorted non-spherically symmetric sites possessing large C_Q. [32-33] The observed value of $C_Q(^{71}Ga)$ = 16.9 MHz for coordination polymer is similar in magnitude to values of $C_Q(^{71}Ga)$ reported for distorted octahedral Ga coordination environments in Ga based MIL-120 and MIL-124 MOFs,[25] coordination complexes [21, 24] and hydroxide cluster compounds.[28] Bonding to different ligands would likely result in different Ga-O bond lengths and distorted octahedral coordination environments. A large value of C_Q is therefore consistent with bonds to multiple types of ligands, such as bridging hydroxyl and acetate ligands. Taken together, the isotropic chemical shift and large C_Q observed for $^{69/71}Ga$ strongly suggests that the Ga coordination environment is a highly distorted 6-coordinate coordination environment.

Description of NMR Experiments on Gallium Oxide. Figure S8 shows the MAS and static ^{71}Ga solid-state NMR spectra of the Ga_2O_3 obtained from thermal treatment of nanobeams. Simulations of ^{71}Ga NMR spectra with parameters previously reported for β-Ga_2O_3 show good agreement with the experimental ^{71}Ga NMR spectra.[8] This is consistent with powder X-ray diffraction which indicates the formation of β -Ga_2O_3 upon heating of the coordination polymer.

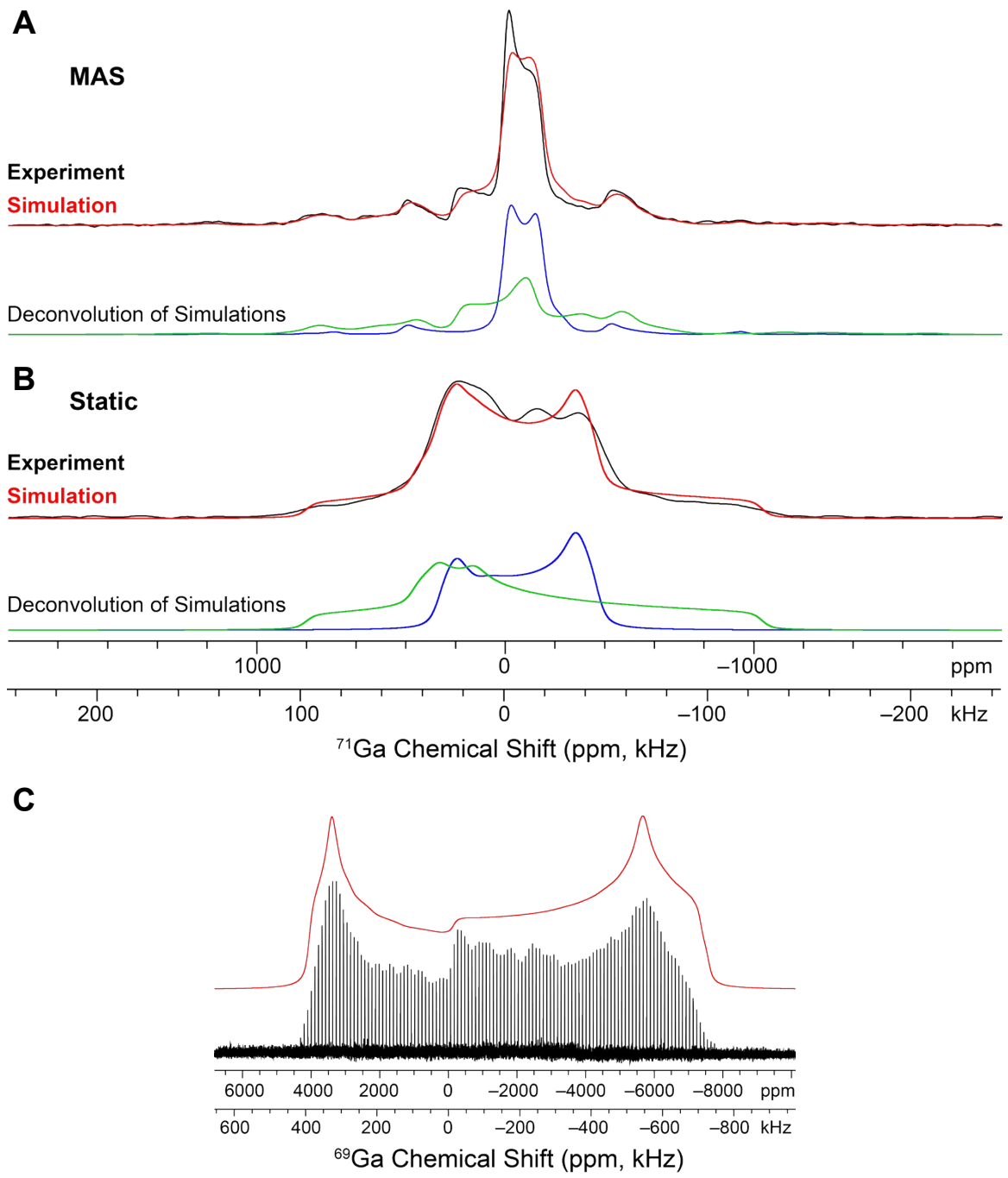

Figure S8. (A) Static ^{71}Ga solid-state NMR spectrum of β-Ga_2O_3 (black traces). The β-Ga_2O_3 was obtained from heat treatment of the coordination polymer derived from etching of EGaIn in 5% acetic acid solution. (B) MAS ^{71}Ga solid-state NMR spectrum acquired with an MAS frequency of 50 kHz. Analytical simulations of the NMR spectra are shown as red traces. The analytical simulations use the ^{71}Ga NMR parameters previously reported for β-Ga_2O_3. Blue and green traces show the simulations of the six-coordinate and four-coordinate Ga sites. (C) Static ^{69}Ga solid-state NMR spectrum of the gallium coordination polymer derived from 5% acetic acid

(black trace) acquired with the WURST-QCPMG pulse sequence and analytical simulation (red trace).

Calculating yield of and wt% of Ga in the heat-treated acetic acid nanobeam

The final product is assumed to be Ga_2O_3 which has a molar mass is given of 187.4 g mol^{-1}. For the predicted structures of the 1D coordination polymer, the molar masses are multiplied by a factor of 2 to compare to the Ga_2O_3 which contains 2 Ga atoms. TGA (Figure 2a) of Ga-based nanobeam resulted in 60% mass of Ga_2O_3.

(1) $2[Ga(\mu\text{-}OH)_2(\mu\text{-}O_2CCH_3)]$

2*(69.7 + 16.0*4 + 1.0*5 + 12*2) = 325.4 g

Wt% Ga = (139.4/325.4)*100 = **42.8%**

Estimated yield of Ga_2O_3 from thermal treatment = (187.4/325.4)*100 = **57.6%**

(2) $2[Ga(\mu\text{-}OH)(\mu\text{-}O_2CCH_3)_2]$

2*(69.7 + 16.0*5 + 1.0*7 + 12*4) = 409.4 g

Wt% Ga = (139.4/409.4)*100 = 34%

Estimated yield = (187.4/409.4)*100 = 45.8%

Table S2. Chemical shift and electric field gradient tensor parameters obtained from simulations of ^{71}Ga and ^{69}Ga static solid-state NMR spectra of the different coordination polymers.

Coordination Polymer	5% Acetic Acid	50% Acetic Acid Solution	Propanoic Acid	Formic Acid Site 1	Formic Acid Site 2
NMR Parameter[a]					
δ_{iso} (ppm)	–15(20)	10(40)	–20(30)	0.0(30)	0.0(50)
C_Q(^{71}Ga)	16.9(3)	21.0(4)	19.0(5)	23.0(5)	14.5(9)
C_Q(^{69}Ga) (MHz)[b]	26.9(3)	33.5(4)	–	36.6(8)	23.0(9)
η_Q	0.14(5)	0.70(5)	0.09(5)	0.6(1)	1.0(1)
Ω (ppm)[c]	340	280	350	200	200
κ [c]	0.53	0.0	–0.42	0.5	0.8
α (°)[c]	–10	0	0	0	0
β (°)[c]	25	0	40	45	30
γ (°)[c]	30	0	60	60	0

[a] The CS tensor is defined by three principal components ordered such that $\delta_{11} \geq \delta_{22} \geq \delta_{33}$, $\delta_{iso} = (\delta_{11} + \delta_{22} + \delta_{33})/3$, $\Omega = \delta_{11} - \delta_{33}$ and $\kappa = 3(\delta_{22} - \delta_{iso})/\Omega$. The EFG tensor is described by three principal components ordered such that $|V_{11}| \leq |V_{22}| \leq |V_{33}|$, $C_Q = eQV_{33}/h$ and $\eta_Q = (V_{22} - V_{11})/V_{33}$. The Euler angles describe the relative orientations of the EFG and CS tensors. Uncertainties in experimental parameters are indicated in parentheses. [b] ^{69}Ga and ^{71}Ga both have $I = 3/2$ and therefore the C_Q values for ^{69}Ga and ^{71}Ga are directly proportional to the quadrupole moment of each nucleus. CQ was accurately determined by simulating spectra from both nuclei simultaneously with the constraint, $C_Q(^{69}\mathrm{Ga}) = \left[Q(^{69}\mathrm{Ga})/Q(^{71}\mathrm{Ga})\right] \times C_Q(^{71}\mathrm{Ga}) = 1.59 \times C_Q(^{71}\mathrm{Ga})$. [c] The uncertainties associated with the CS tensor parameters (Ω and κ) and Euler angles (α, β and γ) are very large (±50%). They were included as adjustable parameters to improve the quality of the simulations. Acquisition of data at higher fields could improve the uncertainties associated with these parameters.

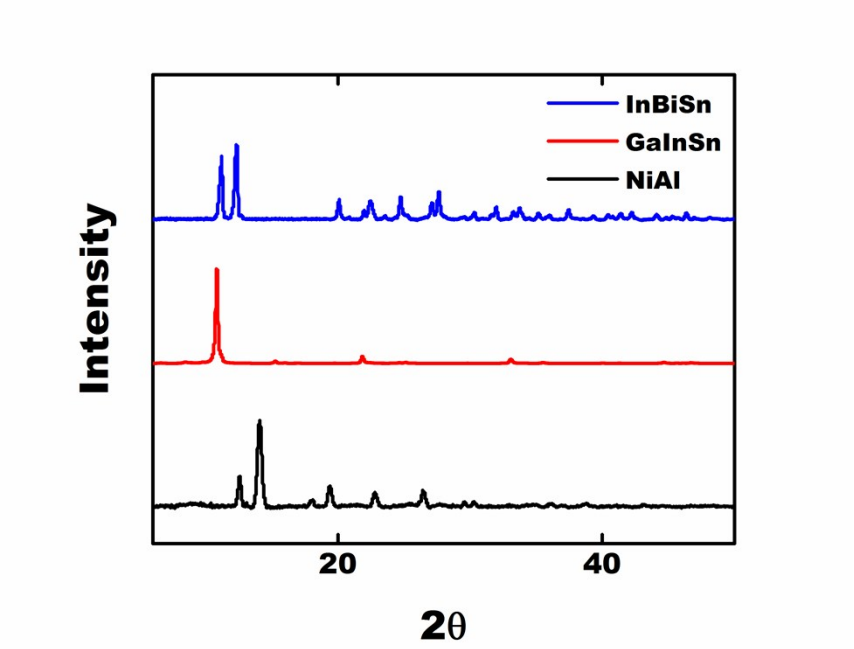

Figure S9. PXRD of coordination polymers synthesized using different alloys in acetic acid. GaInSn and NiAl resulted in the same structure as pure Ga and Al.

Table S3. Distribution of metal center in InBiSn derived coordination polymer from EDS.

Metal atom	Distribution %
In	51.7
Sn	28
Bi	20.3

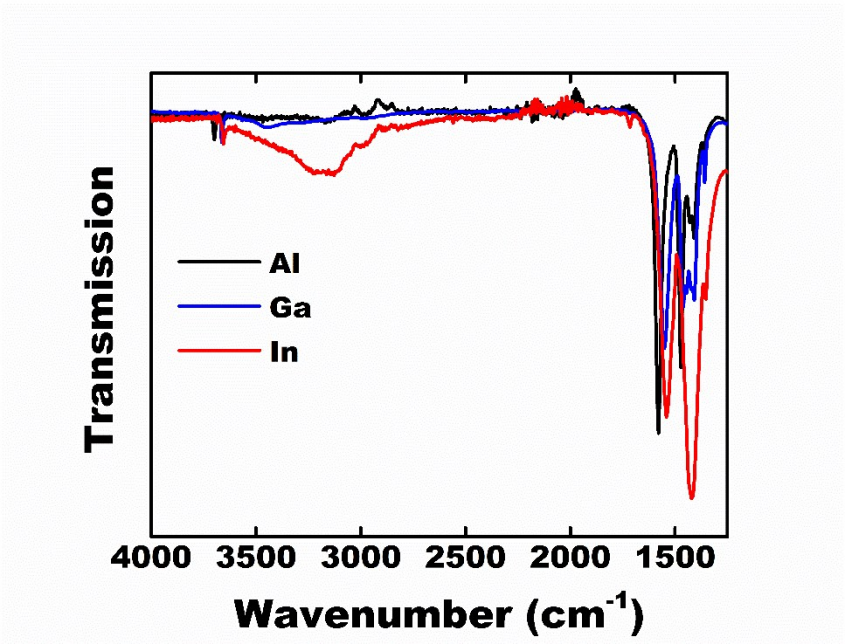

Figure S10. FTIR of coordination polymers synthesized using different metals in acetic acid. Acetate and hydroxyl ligands can be observed in all cases.

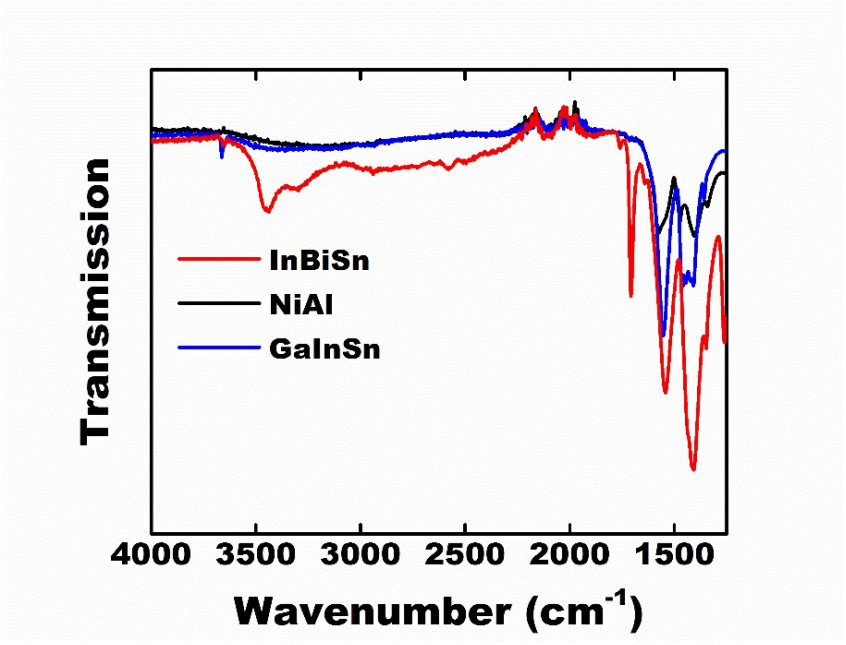

Figure S11. FTIR of coordination polymers synthesized using different alloys in acetic acid. Acetate and hydroxyl ligands can be observed in all cases.

Calculating yield of and wt% of Ga in the heat-treated formic acid nanobeam

The final product is assumed to be Ga_2O_3 which has a molar mass is given of 187.4 g mol^{-1}. For the predicted structures of the 1D coordination polymer, the molar masses are multiplied by a factor of 2 to compare to the Ga_2O_3 which contains 2 Ga atoms. TGA (Figure 6f) of Ga-based formic acid nanobeam resulted in 62% mass of Ga_2O_3.

(1) $2[Ga(\mu\text{-}OH)_2(\mu\text{-}O_2CH)]$

2*(69.7 + 16.0*4 + 1.0*3 + 12) = 297.4 g

Wt% Ga = (139.4/297.4)*100 = **46.9%**

Estimated yield of Ga_2O_3 from thermal treatment = (187.4/297.4)*100 = **63%**

(2) $2[Ga(\mu\text{-}OH)(\mu\text{-}O_2CH)_2]$

2*(69.7 + 16.0*5 + 1.0*3 + 12*2) = 353.4 g

Wt% Ga = (139.4/353.4)*100 = 39.4%

Estimated yield = (187.4/353.4)*100 = 53%

Calculating yield of and wt% of Ga in the heat-treated propionic acid nanobeam

The final product is assumed to be Ga_2O_3 which has a molar mass is given of 187.4 g mol^{-1}. For the predicted structures of the 1D coordination polymer, the molar masses are multiplied by a factor of 2 to compare to the Ga_2O_3 which contains 2 Ga atoms. TGA (Figure S13) of Ga-based propionic acid nanobeam resulted in 42% mass of Ga_2O_3.

(1) $2[Ga(\mu\text{-}OH)_2(\mu\text{-}O_2CCH_2CH_3)]$

2*(69.7 + 16.0*4 + 1.0*7+ 12*3) = 353.4 g

Wt% Ga = (139.4/353.4)*100 = **39.4%**

Estimated yield of Ga_2O_3 from thermal treatment = (187.4/353.4)*100 = **53%**

(2) $2[Ga(\mu\text{-}OH)(\mu\text{-}O_2CCH_2CH_3)_2]$

2*(69.7 + 16.0*5 + 1.0*11 + 12*6) = 465.4 g

Wt% Ga = (139.4/465.4)*100 = 30%

Estimated yield = (187.4/465.4)*100 = 40.2%

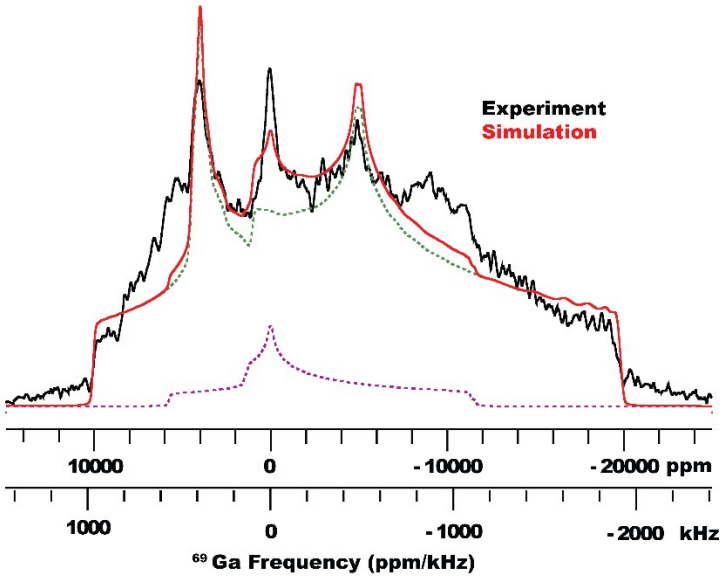

Figure S12. Static ^{69}Ga solid-state NMR spectrum (black trace) and analytical simulation (red trace) for the gallium coordination polymer derived from formic acid. The static ^{71}Ga NMR spectrum is shown in Figure 4g.

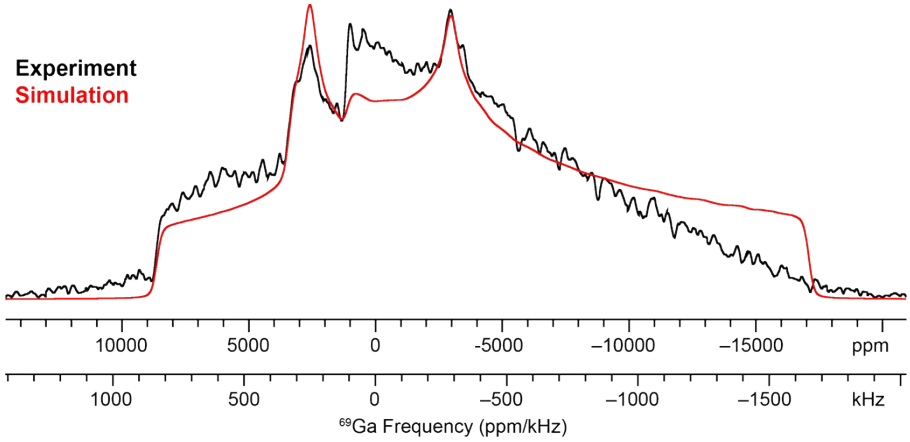

Figure S13. Static ^{69}Ga solid-state NMR spectrum (black trace) and analytical simulation (red trace) for the coordination polymer derived from etching with 50% acetic acid solution. The static ^{71}Ga solid-state NMR spectrum is shown in the main text (Figure 4h).

Supporting Information References:

(1) Harris, R. K.; Becker, E. D.; De Menezes, S. M. C.; Goodfellow, R.; Granger, P., NMR nomenclature. Nuclear spin properties and conventions for chemical shifts (IUPAC Recommendations 2001). *Pure Appl. Chem.* **2001,** *73*, 1795-1818.

(2) Ishii, Y.; Tycko, R., Sensitivity enhancement in solid state N-15 NMR by indirect detection with high-speed magic angle spinning. *J. Magn. Reson.* **2000,** *142*, 199-204.

(3) Metz, G.; Wu, X.; Smith, S., Ramped-Amplitude Cross Polarization in Magic-Angle-Spinning NMR. *J. Magn. Reson. Series A* **1994,** *110*, 219-227.

(4) Marion, D.; Wuthrich, K., Application of phase sensitive two-dimensional correlated spectroscopy (COSY) for measurements of 1H-1H spin-spin coupling constants in proteins. *Biochem. Biophys. Res. Commun.* **1983,** *113*, 967-974.

(5) States, D. J.; Haberkorn, R. A.; Ruben, D. J., A Two-Dimensional Nuclear Overhauser Experiment with Pure Absorption Phase in Four Quadrants. *J. Magn. Reson.* **1982,** *48*, 286-292.

(6) Bhattacharyya, R.; Frydman, L., Quadrupolar nuclear magnetic resonance spectroscopy in solids using frequency-swept echoing pulses. *J. Chem. Phys.* **2007,** *127*, 194503.

(7) O'Dell, L. A.; Schurko, R. W., QCPMG using adiabatic pulses for faster acquisition of ultra-wideline NMR spectra. *Chem. Phys. Lett.* **2008,** *464*, 97-102.

(8) Massiot, D.; Farnan, I.; Gautier, N.; Trumeau, D.; Trokiner, A.; Coutures, J. P., 71Ga and 69Ga nuclear magnetic resonance study of β-Ga2O3: resolution of four- and six-fold coordinated Ga sites in static conditions. *Solid State Nucl. Magn. Reson.* **1995,** *4*, 241-248.

(9) Larsen, F. H.; Jakobsen, H. J.; Ellis, P. D.; Nielsen, N. C., QCPMG-MAS NMR of Half-Integer Quadrupolar Nuclei. *J. Magn. Reson.* **1998,** *131*, 144-147.

(10) Larsen, F. H.; Jakobsen, H. J.; Ellis, P. D.; Nielsen, N. C., Sensitivity-Enhanced Quadrupolar-Echo NMR of Half-Integer Quadrupolar Nuclei. Magnitudes and Relative Orientation of Chemical Shielding and Quadrupolar Coupling Tensors. *J. Phys. Chem. A* **1997,** *101*, 8597-8606.

(11) Lefort, R.; Wiench, J. W.; Pruski, M.; Amoureux, J. P., Optimization of data acquisition and processing in Carr-Purcell-Meiboom-Gill multiple quantum magic angle spinning nuclear magnetic resonance. *J. Chem. Phys.* **2002,** *116*, 2493-2501.

(12) Larsen, F. H.; Skibsted, J.; Jakobsen, H. J.; Nielsen, N. C., Solid-state QCPMG NMR of low-gamma quadrupolar metal nuclei in natural abundance. *J. Am. Chem. Soc.* **2000,** *122*, 7080-7086.

(13) Gan, Z. H.; Amoureux, J. P.; Trebosc, J., Proton-detected N-14 MAS NMR using homonuclear decoupled rotary resonance. *Chem. Phys. Lett.* **2007,** *435*, 163-169.

(14) Hu, B.; Trébosc, J.; Amoureux, J. P., Comparison of several hetero-nuclear dipolar recoupling NMR methods to be used in MAS HMQC/HSQC. *J. Magn. Reson.* **2008,** *192*, 112-122.

(15) Rossini, A. J.; Hanrahan, M. P.; Thuo, M., Rapid Acquisition of Wideline MAS Solid-state NMR Spectra with Fast MAS, Indirect Proton Detection, and Dipolar HMQC Pulse Sequences. *Phys. Chem. Chem. Phys.* **2016,** *18*, 25284-25295.

(16) Brinkmann, A.; Kentgens, A. P. M., Proton-selective O-17-H-1 distance measurements in fast magic-angle-spinning solid-state NMR spectroscopy for the determination of hydrogen bond lengths. *J. Am. Chem. Soc.* **2006,** *128*, 14758-14759.

(17) Dobson, K. D.; McQuillan, A. J., In situ infrared spectroscopic analysis of the adsorption of aliphatic carboxylic acids to TiO2, ZrO2, Al2O3, and Ta2O5 from aqueous solutions. *Spectrochim. Acta, Part A* **1999,** *55*, 1395-1405.

(18) Clausen, M.; Ohman, L. O.; Kubicki, J. D.; Persson, P., Characterisation of gallium(III)-acetate complexes in aqueous solution: A potentiometric, EXAFS, IR and molecular orbital modelling study. *J. Chem. Soc., Dalton Trans.* **2002**, 2559-2564.

(19) Cademartiri, L.; Thuo, M. M.; Nijhuis, C. A.; Reus, W. F.; Tricard, S.; Barber, J. R.; Sodhi, R. N. S.; Brodersen, P.; Kim, C.; Chiechi, R. C.; Whitesides, G. M., Electrical Resistance of AgTS-S(CH2)n-1CH3//Ga2O3/EGaIn Tunneling Junctions. *J. Phys. Chem. C* **2012,** *116*, 10848-10860.

(20) Mensinger, Z. L.; Zakharov, L. N.; Johnson, D. W., Synthesis and Crystallization of Infinite Indium and Gallium Acetate 1D Chain Structures and Concomitant Ethyl Acetate Hydrolysis. *Inorg. Chem.* **2009,** *48*, 3505-3507.
(21) Massiot, D.; Vosegaard, T.; Magneron, N.; Trumeau, D.; Montouillout, V.; Berthet, P.; Loiseau, T.; Bujoli, B., 71Ga NMR of reference GaIV, GaV, and GaVI compounds by MAS and QPASS, extension of gallium/aluminum NMR parameter correlation. *Solid State Nucl. Magn. Reson.* **1999,** *15*, 159-169.
(22) Ash, J. T.; Grandinetti, P. J., Solid-state NMR characterization of 69Ga and 71Ga in crystalline solids. *Magn. Reson. Chem.* **2006,** *44*, 823-831.
(23) Taulelle, F.; Maquet, J.; Lucas, V.; Thery, J.; Kahn-Harari, A.; Faltens, T.; Dunn, B., 71Ga,27Al and 23Na solid state MAS NMR of β- and β″-aluminogallates. *Appl. Magn. Reson. 4*, 101-120.
(24) Fredoueil, F.; Bujoli, B.; Fredoueil, F.; Massiot, D.; Poojary, D.; Clearfield, A.; Bujoli-Doeuff, M., 71Ga and 31P solid state NMR: a powerful tool for the characterization of the first gallium phosphonates. *Chem. Commun.* **1998**, 175-176.
(25) Hajjar, R.; Volkringer, C.; Loiseau, T.; Guillou, N.; Marrot, J.; Férey, G.; Margiolaki, I.; Fink, G.; Morais, C.; Taulelle, F., 71Ga Slow-CTMAS NMR and Crystal Structures of MOF-Type Gallium Carboxylates with Infinite Edge-Sharing Octahedra Chains (MIL-120 and MIL-124). *Chem. Mater.* **2011,** *23*, 39-47.
(26) Martineau, C.; Loiseau, T.; Beitone, L.; Ferey, G.; Bouchevreau, B.; Taulelle, F., Single-crystal XRD and solid-state NMR structural resolution of a layered fluorinated gallium phosphate: RbGa3(PO4)2(HPO4)F4[middle dot]C5N2H16[middle dot]2H2O (MIL-145). *Dalton Trans.* **2013,** *42*, 422-431.
(27) O'Dell, L. A.; Schurko, R. W., QCPMG using adiabatic pulses for faster acquisition of ultra-wideline NMR spectra. *Chem. Phys. Lett.* **2008,** *464*, 97-102.
(28) Ma, Z. L.; Wentz, K. M.; Hammann, B. A.; Chang, I. Y.; Kamunde-Devonish, M. K.; Cheong, P. H.-Y.; Johnson, D. W.; Terskikh, V. V.; Hayes, S. E., Solid-State 69Ga and 71Ga NMR Study of the Nanoscale Inorganic Cluster [Ga13(μ3-OH)6(μ2-OH)18(H2O)24](NO3)15. *Chem. Mater.* **2014,** *26*, 4978-4983.
(29) Schurko, R. W., Ultra-Wideline Solid-State NMR Spectroscopy. *Acc. Chem. Res.* **2013,** *46*, 1985-1995.
(30) Gan, Z.; Amoureux, J. P.; Trébosc, J., Proton-detected 14N MAS NMR using homonuclear decoupled rotary resonance. *Chem. Phys. Lett.* **2007,** *435*, 163-169.
(31) Rossini, A. J.; Hanrahan, M. P.; Thuo, M., Rapid acquisition of wideline MAS solid-state NMR spectra with fast MAS, proton detection, and dipolar HMQC pulse sequences. *Phys. Chem. Chem. Phys.* **2016,** *18*, 25284-25295.
(32) Ashbrook, S. E.; Duer, M. J., Structural information from quadrupolar nuclei in solid state NMR. *Concepts Magn. Reson., Part A* **2006,** *28A*, 183-248.
(33) Kentgens, A. P. M., A practical guide to solid-state NMR of half-integer quadrupolar nuclei with some applications to disordered systems. *Geoderma* **1997,** *80*, 271-306.